HHS Public Access

Author manuscript

Min Metall Explor. Author manuscript; available in PMC 2022 August 16.

Published in final edited form as:

Min Metall Explor. 2020 April 14; 37(4): 1065–1078. doi:10.1007/s42461-020-00209-6.

Characterization of Aerosols in an Underground Mine during a Longwall Move

Aleksandar D. Bugarski[1], **Jon A. Hummer**[1], **Shawn Vanderslice**[1], **Michael R Shahan**[1]

[1]National Institute for Occupational Safety and Health, Pittsburgh Mining Research Division, 626 Cochrans Mill Rd., Pittsburgh, PA 15236, USA

Abstract

A study was conducted in an underground mine with the objective to identify, characterize, and source apportion airborne aerosols at the setup face and recovery room during longwall move operations. The focus was on contributions of diesel- and battery-powered heavy-duty vehicles used to transfer equipment between the depleted and new longwall panels and diesel-powered light-duty vehicles used to transport personnel and materials to various locations within the mine. Aerosols at the setup face were found to be distributed among diesel combustion-generated submicrometer and mechanically generated coarse aerosols. According to the data, the submicrometer aerosols downstream of the setup face were sourced to diesel exhaust emitted by vehicles operated inside and outside of the panel. Depending on the intensity of the activities on the panel, the outby sources contributed between 12.5 and 99.6% to the average elemental carbon mass flow at the setup face and recovery room. Extensively used light-duty vehicles contributed measurably to the elemental carbon concentrations at the setup face. The number concentrations of aerosols downstream of the setup face were associated with aerosols generated by combustion in diesel engines operated in the shield haulage loop and/or outside of the longwall panels. Entrainment of road dust by diesel or battery-powered load-haul-dump vehicles operated near the measurement site appears to be the primary source of mass concentrations of aerosols. The findings of this study should help the underground mining industry in its efforts to reduce exposures of miners to diesel and coarse aerosols.

Keywords

Aerosols; Diesel; Dust; Underground mining; Longwall

1 Introduction

Occupational exposures to respirable dust and submicrometer aerosols emitted by diesel-powered equipment are a health concern for underground mining operators and

✉Aleksandar D. Bugarski, abugarski@cdc.gov.

Conflict of Interest All authors declare that they have no conflict of interest.

Compliance with Ethical Standards

Disclaimer The findings and conclusions in this manuscript are those of the authors and do not necessarily represent the views of the National Institute for Occupational Safety and Health (NIOSH) and the Center for Disease Control and Prevention (CDC). Mention of company names or products does not constitute endorsement by NIOSH or CDC.

regulators [1, 2]. Exposure to various types of respirable dust has been linked to lung diseases including silicosis, coal workers' pneumoconiosis, progressive massive fibrosis, emphysema, and chronic bronchitis [3, 4]. Long-term occupational exposure to diesel exhaust has been found to result in adverse pulmonary, cardiovascular, and other health outcomes [5–9]. In 2012, the International Agency for Research on Cancer (IARC) classified diesel exhaust as a group 1 carcinogen [10].

Aerosols in underground mining operations can be traced back to various mechanical and combustion processes [11, 12]. Comminution and entrainment of road dust are the sources of coarse aerosols in underground coal [12, 13] and metal mines [14–16]. Where used, diesel engines contribute to concentrations of submicrometer aerosols in underground mines [14, 17–19]. In some cases, submicrometer aerosols in underground mines could be traced to various non-diesel-related sources introduced to the workings via ventilation systems such as explosions [14], welding, drilling [15], cigarette smoking [15], general area pollution [13], forest fires, or intake air heating processes.

A large number of diesel engines of various vintages are currently used in underground mines in the USA and around the world [20, 21]. In general, these engines meet a variety of superseded and current emission standards [22–24] and contribute differently to the concentrations of submicrometer aerosols in the underground environment [19, 25–27]. Technologyforcing emission regulations, promulgated over the past few decades [22–24], stimulated dramatic advancements in diesel engine and exhaust aftertreatment technologies. Those advancements resulted in major reductions in emission levels and changes in the properties of emitted aerosols [28–30]. However, due to good durability, low maintenance costs, availability of rebuild programs, and potentially some regulatory and economic factors, older technology engines are currently a preferred source of power for underground mining fleets [31] and could remain so for some time.

The concentrations of submicrometer aerosols and levels of exposures of underground miners to diesel aerosols vary widely among operations [5, 32]. Analysis of samples collected by the Mine Safety and Health Administration (MSHA) in the US underground metal, non-metal, and stone mines between 2012 and 2016 shows that the average exposures to total carbon (TC) and elemental carbon (EC) of miners [32, 33] have been below the current 160 $\mu g_{TC}/m^3$ personal exposure limit [2]. However, the same set of data shows frequent diesel particulate matter (DPM) overexposures of particular occupations, such as blasters, drillers, and scalers, in some segments of the industry. A few studies [12, 14, 15] reported the actual concentrations, size distributions, and chemical composition of the submicrometer aerosols in specific underground workings for actual production scenarios. Additional information is needed on concentrations, properties, and sources of ever-evolving aerosols produced by underground mining processes supported by diesel-powered vehicles in order to assist efforts on reducing exposure of underground miners to diesel aerosols.

This study was conducted to identify, characterize, and source apportion airborne aerosols at the setup face and recovery room of an underground mine during longwall move operations. The primary focus was on aerosols generated by diesel- and battery-powered heavy-duty (HD) vehicles used to transfer equipment between the mined and new longwall panels and

diesel-powered light-duty (LD) vehicles used to transport personnel and materials to various locations within the mine.

2 Methodology

2.1 Site

The experimental work was conducted at an underground mine where the active production at the room-and-pillar and longwall sections has been done predominantly by using electrically powered equipment with product haulage executed by a conveyor belt. The diesel-powered fleet of over 250 permissible HD [34], non-permissible HD [35], and non-permissible LD [35] diesel-powered vehicles are primarily used to transport equipment, material, and personnel. The periodic moves of massive longwall equipment, including shearer, shields, conveyor belt components, and power stations from the recovery room at the mined panel to the setup face at the next panel, require extensive use of diesel-powered equipment (Fig. 1). Those activities, when compared with normal production activities when fewer diesel-powered equipment are used, have higher potential to generate submicrometer aerosols.

The results of sampling and measurements performed for six 2-hour test periods during the day shifts for three consecutive days (D1, D2, and D3) are examined in this study. Two of those tests were conducted on D1 (D1T1 and D1T2), two on D2 (D2T1 and D2T2), and two on D3 (D3T1 and D3T2). Sampling and measurements were performed at three locations: (1) FA0, (2) REC, and (3) SUF (Fig. 1). Those locations were selected to allow for (1) identification and characterization of aerosols at various workplaces and (2) source apportioning of aerosols to activities of various diesel-powered vehicles operated outby and inby of the panels. For the purpose of this study, only area samples were collected; therefore, the observed concentrations cannot be interpreted as personal exposure levels.

The longwall move operations were ventilated with fresh air supplied from two ventilation shafts via main drifts east of the new panel, and four main drifts were used to access and ventilate the new panel (rooms “1”, “2”, “3”, and “0” in Fig. 1). The operation was executed in two different air splits used to ventilate: (1) the longwall section on the new panel and (2) the recovery room on the mined panel (Fig. 1). The contaminated air was exhausted from the new panel via a regulator located at the south end of SUF.

The ventilation flow rates at the sampling stations, FA0 (Q_{FA0}), REC (Q_{REC}), and SUF (Q_{SUF}), were estimated from periodic measurements of the air velocities. Due to the intense traffic flow, it was impossible to obtain air velocities in the drift leading to the recovery room, so the airflow rates were calculated by using the assumption that those were identical in all four entries leading to the panel and by applying the conservation of mass principle ($Q_{REC}=4*Q_{FA0}-Q_{SUF}$). The velocities were measured using DA400 rotating vane anemometers from Pacer Instruments (Keene, NH, USA). The data was collected at a frequency of 0.1 Hz, using CR1000 data loggers from Campbell Scientific (Logan, UT, USA).

The cross-sectional areas of the openings at FA0 and SUF were measured to be 12.1 m^2 (130 ft^2) and 8.8 m^2 (95 ft^2), respectively. The average ventilation flow rates at FA0 for D1T1, D1T2, D2T1, D2T2, D3T1, and D3T2 were calculated to be approximately 13.86 ± 0.50 m^3/s (~ 29,400 ± 1100 ft^3/min). The average ventilation flow rate at SUF was calculated to be approximately 26.05 ± 0.54 m^3/s (~ 55,200 ± 1200 ft^3/min) for D1T1, D1T2, D2T1, and D2T2 and 33.20 ± 0.23 m^3/s (~ 70,300 ± 500 ft^3/min) for D3T1 and D3T2. The average ventilation flow rate at REC was calculated to be approximately 29.39 ± 2.06 m^3/s (~ 62,300 ± 4400 ft^3/min) for D1T1, D1T2, D2T1, and D2T2 and 22.25 ± 2.06 m^3/s (~ 47,200 ± 4300 ft^3/min) for D3T1 and D3T2.

2.2 Vehicles and Fuel

During the longwall move, a small fleet of permissible and non-permissible diesel-powered HD vehicles and a single battery-powered HD vehicle hauled shields from the recovery room at the depleted panel to the setup face on the new panel (Fig. 1). The total shield haulage distance was over 3219 m (2 miles). Concurrently, a number of other diesel-powered HD vehicles moved belt components and power equipment from the recovery room to the various locations on the new longwall section. A number of LD diesel-powered vehicles were used to transport personnel and materials and to perform various supporting tasks on the same section. More discussion on the role of different groups of the vehicles in the longwall move is provided in the Results and Discussion section.

All diesel-powered vehicles used in the longwall move were fueled from a single batch of the ultralow sulfur diesel (ULSD) fuel. A 2-L sample of the fuel was collected from the supply tank and sent for selected analyses to Bureau Veritas of North America (Houston, TX, USA). The results of the analyses are shown in Table 1.

2.3 Vehicle Activity

The activities of vehicles used during selected intervals of the longwall move were monitored at seven locations distributed across the panels (Fig. 2). The monitoring stations were strategically located along the recovery room loop (REC loop), shield hauler loop, and setup face loop (SUF loop) (Fig. 2). The data was used to (1) identify vehicles that were operated during the study, (2) to assess the extent of the utilization of the HD and LD vehicles on different sections, and (3) based on ventilation air flow distribution, to apportion aerosols to the various activities and categories of the diesel-powered vehicles.

The movement of vehicles in the split of air that was used to ventilate the recovery room (Fig. 1) was captured from the stations nos.1, 2, and 3. The concentrations of diesel aerosols at REC were attributed to the activities of the vehicles in the REC loop. The concentrations of diesel aerosols at SUF were attributed to the activities of the vehicles in the shield hauler and SUF loops. The stations nos. 2, 3, 6, and 7 were used to record the movement of vehicles within the shield hauler loop (Fig. 2). The stations nos. 4, 5, and 6 were used to log the movement of vehicles on the SUF loop (Fig. 2).

2.4 Sampling, Analysis, and Measurements

Sampling and measurements were performed at (1) FA0 located in “0” room of the new longwall section, 50 m (164 ft) downwind of the fresh air split; (2) SUF located 20 m (66 ft) upwind of the regulator; and (3) REC located 150 m (492 ft) upwind of the entrance to the recovery room (Fig. 2).

The effects of the longwall move process on the submicrometer and respirable aerosols were studied in relation to the results of various analyses performed on the filter samples and the results of measurements with direct reading instruments. Triplicate filter samples of submicrometer and respirable aerosols were collected at FA0, REC, and SUF for carbon analysis, using the identical custom-made sampling systems (Fig. 3). The submicrometer aerosol samples were collected on tandem 37-mm quartz fiber filters (QFFs) enclosed in DPM cassettes (SKC, Eighty Four, PA, Model 225–317) exclusively used for compliance sampling in underground mines in the USA [36]. The respirable aerosol samples for carbon analysis were collected on pre-baked tandem 38-mm QFFs (Pall Life Sciences, Ann Arbor, MI, QAT2500), assembled in 5-piece cassettes (SKC 225–3050LF + SKC 225–304). The 10-mm Dorr-Oliver cyclones (Zefon, Ocala, FL, Model 456243) were used to eliminate the majority of coarse aerosols from the submicrometer and respirable samples. The nominal sampling flow rates of 1.7 lpm were maintained by subsonic critical orifices, which were installed in the manifolds coupled to a single vacuum pump (Oerlikon Leybold Vacuum GmbH, Cologne, Germany, Sogevac SV25B). The actual sampling flow rates were determined using results of flow verifications performed before and after each test using a primary flow calibrator (Mesa Laboratories, Lakewood, CO, Bios Defender 530).

Submicrometer and respirable aerosol samples collected on QFF media were analyzed in-house for EC and organic carbon (OC) using a thermo-optical transmittance (TOT) following NIOSH Method 5040 [37]. Results of the analysis performed on the secondary filters were used to make dynamic blank correction for the primary filters. Due to uncertainty associated with high OC contamination of the QFF media in the DPM cassettes and short sampling times, only EC data were reported.

An electrical low-pressure impactor (ELPI) from Dekati (Tampere, Finland) [38, 39] was used at SUF to do real-time measurements of concentrations and size distributions of aerosols. The ELPI is a 13-stage impactor with nominal cut sizes ($_{50}D_{ae}$) of 29 nm, 58 nm, 102 nm, 165 nm, 254 nm, 391 nm, 635 nm, 990 nm, 1.60 μm, 2.45 μm, 3.96 μm, 6.67 μm, and 10.12 μm. In the configuration used in this study, a filter stage is added after the 29-nm stage to capture aerosols below that size. The filter stage has a broad lower cutoff in the 5- to 10-nm range. A response in the order of seconds makes this instrument suitable for monitoring rapidly changing distributions. The ELPI is used with 25-mm, greased aluminum foil substrates that were changed frequently to avoid overloading.

A single personal dust monitor PDM3600 (Thermo Fisher Scientific, Franklin, MA) was used at each measurement location to continuously measure ambient concentrations of dust. The PDM is designed for continuous monitoring of exposure of underground coal miners to respirable dust [40, 41] and uses a Higgins-Dewell cyclone (nominal median cut point of 4.0

μm) at the inlet to eliminate coarse dust from the respirable sample. In this study, a sampling flow rate of 2.2 l/min was used.

3 Results and Discussion

3.1 Vehicles Used During Longwall Move

The vehicle monitoring showed intermittent use of six diesel-powered HD vehicles (Table 2) and one battery-powered HD vehicle. The permissible diesel-powered load-haul-dump (LHD) vehicle V1 (Table 2), powered by an MSHA-approved engine and fitted with filtration systems with disposable filter elements (DFEs) [42], was used to move shields from the recovery room to the transfer points next to the “0” room (Fig. 1) during D1T1, D1T2, D2T1, and D2T2 tests. During D3T1 and D3T2 tests, the same vehicle moved shields delivered by the shield haulers to the transfer point in “2” room to the setup face. During D1T1, D1T2, D3T1, and D3T2 tests, two non-permissible HD vehicles, V2 and V3 (Table 2), were utilized to transport the shields from the transfer point in the “0” room outside of the recovery room to the transfer point in the “2” room outside of the setup face. These vehicles were powered by US EPA Tier 3 engines and retrofitted with sintered metal filter systems (HJS, SMF-AR) [43]. During D2T1 and D2T2 tests, the crew performed the maintenance on one of the shield haulers, and only LD diesel-powered vehicles were operated at the SUF loop. The shield haulers moved the empty trailers back to the transfer point in the “0” room via the “2” room. During D1T1, D1T2, D2T1, and D2T2 tests, the battery-powered permissible LHD vehicle was used to move shields from the transfer point in “2” room to the setup face. To move other heavy equipment throughout the panels, the following pieces of equipment were intermittently used: a permissible LHD V4, powered by an MSHA-approved engine and fitted with a filtration system with DFEs; a non-permissible LHD V5, powered by US EPA Tier 3 engine fitted with diesel oxidation catalytic converter (DOC); and a non-permissible LHD V6, powered by an MSHA-approved engine fitted with a DOC.

The movement of over 40 LD vehicles was logged during the tests. The LD fleet consisted of various kinds of personnel and material carriers, three forklifts, and one water truck. These were powered by a variety of diesel engines with outputs between 15 (20 hp) and 164 kW (220 hp). All were engines of various vintages and certified by MSHA [22] or the US EPA [23]. Due to the large representation, movements of LD vehicles were not individually studied. However, three general trends were observed: (1) the LD traffic occurred primarily in “2” room, between the entrance to the panel and entrance to the SUF loop; (2) the LD traffic in “0” room, which was almost exclusively used by loaded shield haulers, was sparse; and (3) the LD vehicles were primarily used for transportation of crew members and supervisors.

3.2 EC Concentrations at SUF and REC

The results of EC carbon analysis performed on submicrometer aerosol samples, normalized with the maximum concentration observed for all tests are summarized in Fig. 4a. Those results show that the concentrations of submicrometer aerosols at REC were a mixture of those generated by HD and LD vehicles operated within the area upstream of the REC

sampling station (Fig. 1) and those brought by ventilation air from the areas outby the FA0 sampling station. The concentrations of submicrometer aerosols at SUF appear to be a mixture of those generated by vehicles operated within the shield hauler and SUF loops and those brought by ventilation air from the areas outby the FA0 sampling station. Due to the long air travel time between outby boundaries of the shield haulage loop and SUF (estimated to be approximately 2400 s), the vehicles in operation on that air split before and during specific test times could contribute to the measured concentrations.

The EC mass flow rates for FA0, REC, and SUF were calculated using the results of EC concentration and average ventilation flow rate measurements at respective locations. The analysis of EC mass flow rates showed that submicrometer aerosols at the REC and SUF were generated by (1) activities of various diesel-powered vehicles operated outby of the panels and (2) activities of diesel-powered vehicles operated on the panels. The EC concentrations and relative contributions of inby and outby diesel activities to the EC mass rates at REC and SUF varied widely between tests. During the D1T1, D1T2, and D2T2 tests, the diesel-powered vehicles were extensively used inside the REC loop (Fig. 2), and the EC mass rates at the REC were higher than during the D2T1, D3T1, and D3T2 tests (Fig. 4a). Similarly, the more extensive use of the diesel-powered vehicles inside the shield hauler and SUF loops (Fig. 2) during the D2T2, D3T1, and D3T2 tests (by comparison to the D1T1, D1T2, and D2T1 tests) resulted in higher EC mass flows at SUF (Fig. 4a). The data suggests that the outby traffic contributed between 12.5 and 99.6% to the average EC mass flow at REC and SUF (Fig 4b). During the tests with limited usage of diesel-powered equipment inside of the REC shield haulage or SUF loops, the background was the primary contributor to the total EC mass flow for corresponding locations. The outby traffic EC mass flow contributed at least one-third of the total EC mass flow at REC for tests D2T1, D2T2, D3T1, and D3T2 (Fig. 4b). Similarly, the outby traffic contributed between 38 and 60% to the average EC mass flow at SUF for tests D1T1, D1T2, and D2T1 (Fig. 4b). Even in the cases of tests when diesel-powered vehicles were used extensively within the panel, the outby traffic contributed at least 12% of the total EC mass at REC and SUF (Fig. 4b).

3.3 Number and Mass Concentrations of Aerosols at SUF

The results of continuous measurements of aerosol concentrations with the ELPI during six tests were used to study the effects of the longwall move process on the number and mass concentrations and size distributions of aerosols at SUF. The traces of number and mass concentrations for individual tests, normalized with the maximum corresponding concentrations observed for all tests, are shown in Fig. 5. The average normalized number and mass concentrations for all six individual tests are shown in Fig. 6a.

The number and mass concentrations fluctuated widely within and among the tests (Fig. 5 and Fig. 6a). The vehicles that were operated over sporadic and transient duty cycles produced wide ranges of number and mass concentrations. In the case of the D1T1 test, activities of the sintered metal filter equipped shield haulers and the few LD vehicles on the shield haulage loop resulted in the low EC mass flow (Fig. 4) and low number concentrations (Figs. 5a and 6a). However, concurrent activities of the battery-powered LHD at the setup face loop produced high mass concentrations of aerosols (Fig. 6b). For all

other tests, the elevated mass concentrations generally coincided with the elevated number concentrations (Fig. 5), indicating that diesel-powered vehicles were often not only the primary source of submicrometer aerosols but were also a primary source of entrained coarse dust. The spikes of number and mass concentrations, most evident for certain parts of the D1T2 and D3T2 tests (Fig. 5b and f), were associated with operation of diesel-powered vehicles in the room behind and parallel to the setup face room (Fig. 1). In the case of the D1T2 test, a personnel carrier powered by a modern engine was used in the aforementioned area in the period between 600 and 1200 s. In the case of the D3T2 test, the LHD V6 (Table 2) powered by a high-emitting engine [42] was brought in shortly after the start of the test and operated in a repeatable fashion over a transient cycle for approximately 1200 s (Fig. 5f). The number concentrations at the SUF were partially associated with aerosols generated by diesel engines operated at the shield haulage loop and/or outside of the longwall panels. The spikes in number and mass concentrations of aerosols downstream of the setup face were associated with operation of diesel-powered vehicles near the measurement site. High instantaneous mass concentrations were primarily associated with entrainment of the dust by diesel- or battery-powered LHD vehicles operated close to SUF, at the setup face, or in the room behind the setup face (Fig. 1).

3.4 Size Distributions of Aerosols at SUF

The number and mass size distributions for selected instances of the six tests, normalized with the respect to the highest corresponding number and mass concentrations observed during those tests, are shown in Figs. 7 and 8, respectively. The statistical parameters for those distributions are provided in Tables 3 and 4, respectively. In general, the aerosols were distributed among two, three, or even four log-normal modes (Figs. 7 and 8). The combustion-generated aerosols dominated the number distributions. Those were distributed between two submicrometer modes (Table 3): (1) aged agglomeration mode aerosols with count median diameters (CMDs) between 160 and 210 nm and (2) freshly generated nucleation and agglomeration mode aerosols with CMDs between 27 and 166 nm. The contemporary engine in the personnel carrier that was operated in the vicinity of SUF was the primary source of the nucleation and agglomeration mode aerosols with CMDs below 81 nm recorded in a few instances (1174 and 5163 s) during the D1T2 test (Fig. 7b). In the case of D3T2, the older technology engine in the LHD V6 (Table 2) was the primary source for a few spikes of a high number concentration of aerosols with CMDs around 160 nm. The mode with mechanically generated coarse aerosols that were present in several orders of magnitude lower number concentrations than combustion-generated aerosols was not discernable (Table 3).

In the majority of cases, aerosols were distributed by mass in a single coarse mode consisting of dust entrained by vehicles and equipment operated in the vicinity of the measurement sites (Fig. 8 and Table 4). The mass median diameters (MMDs) of entrained dust were between 2.6 and 31.5 μm. In some cases, the combustion aerosols exhibited a discernable secondary mass mode (Fig. 8 and Table 4) and contributed to the overall mass of aerosols (Table 4). For example, at 1174 s of the D1T2 test, the activities at the setup face were low, and the submicrometer aerosol with MMDs of 360 nm evidently contributed to the total mass of aerosols (Table 4). It is important to note that the majority of the MMDs for

coarse modes was not measured but assessed mathematically by fitting log-normal curves to the existing data and extrapolating those outside of the measurement range of the ELPI using DistFit™ 2009 (Chimera Technologies, Inc., Forest Lake, MN, USA).

The activities of vehicles operated at and outside of the panel had an impact on number, mass concentrations, and size distributions of aerosols at SUF. The number concentrations was found to be the highest when diesel-powered vehicles were operated close to SUF (Fig. 5b and f). The number of distributions of aerosols at SUF was found to be single or bimodal. In a majority of the cases, the distributions were bimodal as follows: (1) one mode was apparently made of “fresh aerosols” generated by individual vehicles operated in the vicinity of SUF, and (2) the second mode apparently was made of the “aged aerosols” contributed by vehicles operated at outby sections or outside of the panel and transformed on their journey to SUF.

Dominant single modal distributions were observed for two scenarios: (1) the individual diesel-powered vehicle operated in the vicinity of SUF contributed to the high number of aerosols (e.g., Figs. 5b and 7b for 1174 and 5163 s and Figs. 5f and 7f for 762 s), and (2) the vehicles operated in the outby sections or outside of the panel were a primary source of submicrometer aerosols (e.g., Figs. 5c and 7c for 5579 and 6656 s and Figs. 5d and 7d for 2697 and 5909 s).

Mass concentrations were primarily associated with entrainment of dust by the diesel-powered or battery-powered LHD vehicle operated at the setup face or the drift behind the setup face. The distributions of aerosols mass were single modal or sometimes bimodal. The MMDs for entrained dust at SUF were between 17 and 32 μm.

3.5 Mass Concentrations of Respirable Aerosols at FA0, REC, and SUF

The average mass concentrations of respirable aerosols at FA0, REC, and SUF, normalized with the respect to the highest value observed during those tests, were calculated from measurements made with a single PDM at each of those locations (Fig. 9). Measurements were performed from the same general area from which filter samples for carbon analysis were collected and ELPI measurements were made (SUF only).

Entrainment of roadway dust by vehicles operated outside of the panel was the primary contributor to mass concentrations of respirable aerosols at FA0. Those concentrations varied between and during the tests (Figs. 9 and 10). Similarly, entrainment of the roadway dust by HD vehicles operated at the recovery loop was the primary contributor to mass concentrations of respirable aerosols at REC. The concentrations were the highest at REC for the D1T1 and D1T2 tests, when the majority of the equipment was being moved from the recovery room to the transfer point. The mass concentrations of respirable aerosols at SUF were primarily the result of the entrainment of the settled dust by HD vehicles operated at the setup face. The highest concentrations were observed for D1T1 when longwall equipment was moved at the setup face by the battery-powered LHD.

3.6 Relationship of Mass Concentrations of Respirable EC, Respirable Aerosols, and Dust at FA0, REC, and SUF

The mass concentrations of EC obtained via carbon analysis performed on the respirable samples, mass concentrations of respirable aerosols obtained by PDM measurements, and mass concentrations of dust estimated from ELPI measurements (only within instrument range) were used to examine the relation among those entities (Fig. 10).

For conditions prevailing at REC, the EC mass concentrations were between 8.9 and 28.7% of respirable dust concentrations measured with the PDM. For conditions prevailing at the SUF, the EC mass concentrations were between 0.4 and 4.4% of sub-10 μm dust concentrations measured with ELPI and 2.7 and 22.9% of respirable dust concentrations measured with the PDM (Fig. 10b). The respirable dust concentrations measured with the PDM were 13.6 and 24.3% of sub-10 μm dust concentrations measured with ELPI.

4 Conclusion

This study identified, characterized, and sourced apportioned airborne aerosols at selected sections of the underground mine during longwall move operation. Diesel combustion and entrainment of road dust were identified as the primary sources of submicrometer and coarse aerosols, respectively. The analysis indicates that reducing concentrations of diesel aerosols on those sections would require concerted efforts devoted to elimination, substitution, and/or control of various sources of diesel aerosols. The data suggests that those reductions could be achieved by controlling diesel exhaust emissions from HD and LD vehicles operated inside and outside of the panel. Efforts to control emissions of aerosols from HD diesel-powered vehicles should be complemented with similar efforts to reduce emissions of diesel aerosols from the large and extensively utilized fleet of LD vehicles that also contributed to the concentrations of submicrometer particles at the longwall section. Suppressing entrainment of road dust by diesel- or battery-powered vehicles could help to reduce mass concentrations of dust on the sections. The findings of this study should help the underground mining industry in its efforts to reduce exposures of miners to diesel and coarse aerosols.

References

1. 70 FR 24875 (2014) Mandatory health Standards - underground coal mines. Code of Federal Regulations Title 30, Part 70. Mine Safety and Health Administration, Department of Labor
2. 66 FR 35518 (2001) Limit on exposure to diesel particulate matter. Code of Federal Regulations Title 30, Part 57.5060. Mine Safety and Health Administration, Department of Labor
3. Attfield MD, Morring K (1992) An investigation into the relationship between coal workers' pneumoconiosis and dust exposure in U.S. coal miners. Am Ind Hyg Assoc J 53(8):486–492. 10.1080/15298669291360012 [PubMed: 1509988]
4. Hnizdo E, Vallyathan V (2003) Chronic obstructive pulmonary disease due to occupational exposure to silica dust: a review of epidemiological and pathological evidence. Occup Environ Med 60:237–243. 10.1136/oem.60.4.237 [PubMed: 12660371]
5. Peters S, de Klerk N, Reid A, Fritischi L, Musk AW, Vermulen R (2017) Quantitative levels of diesel exhaust exposure and the health impact in the contemporary Australian mining industry. Occup Environ Med 74:282–289. 10.1136/oemed-2016103808 [PubMed: 27919060]

6. Attfield MD, Schleiff PL, Lubin JH, Blair A, Stewart PA, Vermeulen R, Coble JB, Silverman DT (2012) The diesel exhaust in miners study: a cohort mortality study with emphasis on lung cancer. J Natl Cancer Inst 104:869–883. 10.1093/jnci/djs035 [PubMed: 22393207]
7. Silverman DT, Samanic CM, Lubin JH, Blair AE, Stewart PA, Vermeulen R, Coble JB, Rothman N, Schleiff PL, Travis WD, Ziegler RG, Wacholder S, Attfield MD (2012) The diesel exhaust in miners study: a nested case-control study of lung cancer and diesel exhaust. J Natl Cancer Inst 104:855–868. 10.1093/jnci/djs034 [PubMed: 22393209]
8. Power MC, Weiskopf MG, Alexeeff SE, Coull BA, Spiro A III, Schwartz J (2011) Traffic-related air pollution and cognitive functions in a cohort of older men. Environ. Health Perspect 119:682–687. 10.1289/ehp.1002767 [PubMed: 21172758]
9. Mills NL, Miller MR, Lucking AJ, Beveridge J, Flint L, Boere AJF, Fokkens PH, Boon NA, Sandstrom T, Blomberg A, Duffin R, Donaldson K, Hadoke PWF, Cassee FR, Newby DE (2011) Combustion-derived nanoparticulate induces the adverse vascular effects of diesel exhaust inhalation. Eur Heart J 32(21):2660–2671. 10.1093/eurheartj/ehr195 [PubMed: 21753226]
10. International Agency for Research on Cancer (2012) Diesel engine exhaust carcinogenic. IARC Press Release No. 213, June 12, World Health Organization. International Agency for Research on Cancer, Lyon, France
11. Cantrell BK, Volkwein JC (2001) Mine aerosol measurement. In: Baron PA, Willeke K (eds) Aerosol measurement. Principles, techniques, and applications. Second edn. John Willey & Sons, Inc, New York, pp 802–805
12. Rubow KL, Marple VA, Tao Y, Liu D (1990) Design and evaluation of a personal diesel aerosol sampler for underground coal mines. Soc Min Eng. AIME Preprint No. 90–132, pp. 5–9
13. Skubacz K, L Wojtecki, Urban P (2017) Aerosol concentration and particle size distributions in underground excavations of a hard coal mine. Int J Occup Safety Ergon 23(3):318–327. 10.1080/10803548.2016.1198553
14. Saarikoski S, Teinila K, Timonen H, Aurela M, Laaksovirta T, Reyes F, Vasques Y, Oyola P, Artaxo P, Pennanen AS, Junttila S, Linnainmaa M, Salonen RO, Hillamo R (2018) Particulate matter characteristics, dynamics and sources in an underground mine. Aerosol Sci Technol 52(1):114–122. 10.1080/02786826.2017.1384788
15. McDonald JD, Zielinska B, Sagebiel JC, McDaniel MR, Mousset-Jones P (2003) Source apportionment of airborne fine particulate matter in an underground mine. J Air Waste Manag Assoc 53:386–395. 10.1080/10473289.2003.10466178 [PubMed: 12708502]
16. Heath Effects Institute (2002) Measuring diesel emissions exposure in underground mines: a feasibility study by Zielinska B, Sagebiel J, McDonald J, Rogers CF, Fujita E, Mousset-Jones P: Heath Effect Institute, Boston, MA pp 181–232
17. Bugarski AD, Schnakenberg GH Jr, Hummer JA, Cauda E, Janisko SJ, Patts LD (2009) Effects of diesel exhaust aftertreatment devices on concentrations and size distribution of aerosols in underground mine air. Environ Sci Technol 43:6737–6743. 10.1021/es-9006355 [PubMed: 19764243]
18. Bugarski AD, Cauda E, Janisko SJ, Hummer JA, Patts LD (2010) Aerosols emitted in underground mine air by diesel engine fueled with biodiesel. J Air Waste Manag Assoc 60:237–244. 10.3155/1047-3289.60.2.237 [PubMed: 20222537]
19. Barski AD, Cauda EG, Janisko SJ, Patts LD, Hummer JA, Terrillion T, Keifer J (2012) Isolated zone evaluation of the Tier 4i engine equipped with SCR system. Proceeding of 14th United States/North American Mine Ventilation Symposium, Salt Lake City, UT, June 17–20, pp. 205–212
20. Mine Safety and Health Administration (2019) National coal diesel inventory. Available at https://www.msha.gov/support-resources/forms-o-nline-filing/2018/05/23/manageupdate-diesel-inventory. Accessed July 23, 2019
21. The Raw Materials Group and Parker Bay Company (2012) Market analysis: underground mining mobile equipment. September. Stockholm, Sweden and Erie, Pennsylvania
22. 66 FR 5704 (2001) Diesel particulate matter-underground areas of underground coal mines. Code of Federal Regulations Title 30 Part 72. Mine Safety and Health Administration, Department of Labor

23. 69 FR 38957 (2004) Control of emissions of air pollution from nonroad diesel engines and fuel; final rule. Code of Federal Regulations Title 40, Parts 9, 69, 80, 86, 89, 94, 1039, 1048, 1051, 1065, and 1068. Environmental Protection Agency
24. Regulation (EU) 2016/1628 of the European Parliament and of the Council of 14 September 2016 on requirements relating to gaseous and particulate pollutant emission limits and type-approval for internal combustion engines for non-road mobile machinery, amending Regulations (EU) No 1024/2012 and (EU) No 167/2013, and amending and repealing Directive 97/68/EC. OJ L 252, 16.9.2016, p. 53–117
25. Bugarski AD, Janisko SJ, Cauda EG, Patts LD, Hummer JA, Westover C, Terrillion T (2014) Aerosols and criteria gases in an underground mine that uses FAME biodiesel blends. Ann Occup Hyg 58(8):971–982. 10.1093/annhyg/meu049 [PubMed: 25060241]
26. National Institute for Occupations Safety and Health: Effectiveness of selected diesel particulate matter control technologies for underground mining applications: isolated zone study, 2003 (2006). By Bugarski AD, Schnakenberg GH Jr., Noll JD, Mischler SE, Patts LD, Hummer JA, Vanderslice SE. (DHHS (NIOSH) Publication No. 2006–126, RI9667). Pittsburgh, PA: U.S. Department of Health and Human Services, Centers for Disease Control and Prevention
27. National Institute for Occupations Safety and Health: Effectiveness of selected diesel particulate matter control technologies for underground mining applications: isolated zone study, 2004 (2006). By Bugarski AD, Schnakenberg GH Jr., Mischler SE, Noll JD, Patts LD, Hummer JA (DHHS (NIOSH) Publication No. 2006–138, RI9668). Pittsburgh, PA: U.S. Department of Health and Human Services, Centers for Disease Control and Prevention
28. Ruehl C, Herner JD, Yoon S, Collins JF, Misra C, Na K, Robertson WH, Biswas S, Chang M-CO, Ayala A (2015) Similarities and differences between “traditional” and “clean” diesel PM. Emiss Control Sci Technol 1:17–23. 10.1007/s40825-0140002-7
29. Khalek IA, Bougher TL, Merritt PM, Zielinska B (2011) Regulated and unregulated emissions from highway heavy-duty diesel engines complying with U.S. Environmental Protection Agency 2007 emissions standards. J Air Waste Manager. Assoc 61:427–442. 10.3155/1047-3289.61.4.427
30. Khalek IA, Blanks MG, Merritt PM, Zielinska B (2015) Regulated and unregulated emissions from modern 2010 emissions-compliant heavy-duty on highway diesel engines. J Air Waste Manager Assoc 65:987–1001. 10.1080/10962247.2015.1051606
31. Bugarski A, Barone T (2016) Controlling exposure of underground coal miners to diesel aerosols. Presentation at 22nd Annual MDEC Conference, Toronto, Ontario, Canada, October 4–6
32. Bugarski AD, Cauda EG, Barone TL, Vanderslice S (2017) Diesel particulate matter exposure and concentration monitoring in underground mines: Practices and challenges. Presentation at 23rd Annual MDEC Conference, Toronto, Ontario, Canada, October 3–5
33. Mine Safety and Health Administration (2019) The DPM personal sampling compliance data. Mine safety and health Administration. Available at https://arlweb.msha.gov/OpenGovernmentData/OGIMSHA.asp. Accessed July 23, 2019
34. 61 FR 55518 (1996) Diesel power packages intended for use in areas of underground coal mines where permissible electric equipment is required. Code of Federal Regulations Title 30, Part 7. Subpart F. Mine Safety and Health Administration, Department of Labor
35. 61 FR 55527 (1996) Nonpermissible diesel-powered equipment; categories. Code of Federal Regulations Title 30, Part 75.1908. Mine Safety and Health Administration, Department of Labor
36. Noll JD, Timko RJ, McWilliams LJ, Hall P, Haney R (2005) Sampling results of the improved SKC® diesel particulate matter cassette. J Occup Environ Hyg 2(1):29–37. 10.1080/15459620590900320 [PubMed: 15764521]
37. National Institute for Occupational Safety and Health (2016) Monitoring diesel exhaust in the workplace. In NIOSH Manual of Analytical Methods (NMAM), Birch EM,5th Edition, Chapter DL, Cincinnati, OH: U.S. Department of Health and Human Services, Centers for Disease Control and Prevention. Available from https://www.cdc.gov/niosh/nmam/pdfs/NMAM_5thEd_EBook.pdf. Accessed 26 Mar 2020
38. Ahlvik P, Ntziachristos L, Keskinen J, Virtanen A (1998) Real time measurement of diesel particle size distribution with an electric low pressure impactor. SAE Technical Paper 980410. 10.4271/980410

39. Keskinen J, Pietarinen K, Lehtimäki M (1992) Electrical low pressure impactor. J Aerosol Sci 23(4):353–360

40. National Institute for Occupational Safety and Health (2006) Laboratory and field performance of a continuously measuring personal respirable dust monitor. Volkwein JC, Vinson RP, Page SJ, McWilliams LJ, Joy GJ, Mischler SE, and Tuchman DP. (DHHS (NIOSH) Publication No. 2006–145, RI 9669). U.S. Department of Health and Human Services, Centers for Disease Control and Prevention. Available at https://www.cdc.gov/niosh/mining/works/coversheet349.html. Accessed 26 Mar 2020

41. 75 FR 17511 (2010). Coal Mine Dust Sampling Devices. Code of Federal Regulations Title 30, Part 74. Mine Safety and Health Administration, Department of Labor

42. Bugarski AD, Schnakenberg GH Jr, Hummer JA, Cauda E, Janisko SJ, Patts LD (2011) Evaluation of high-temperature disposable filter elements in an experimental underground mine. Society for Min. Metal Explor Trans 330:373–382

43. Bugarski AD, Hummer JA, Miller A, Patts LD, Cauda EG, Stachulak JS (2016) Emissions from a diesel engine using Febased fuel additives and sintered metal filtration system. Ann Occup Hyg 60(2):252–262. 10.1093/annhyg/mev071 [PubMed: 26424805]

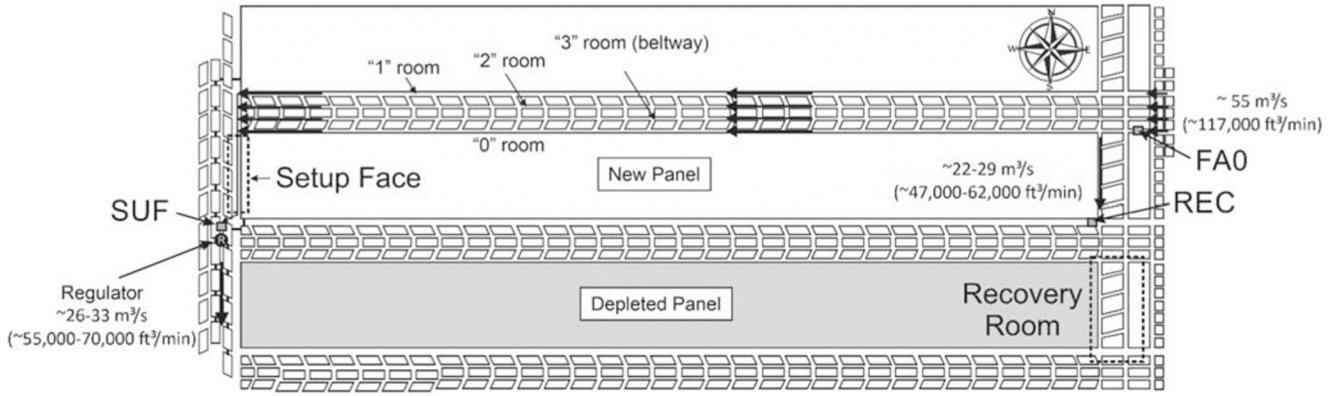

Fig. 1.
Schematic of longwall panels and ventilation concept (not to scale)

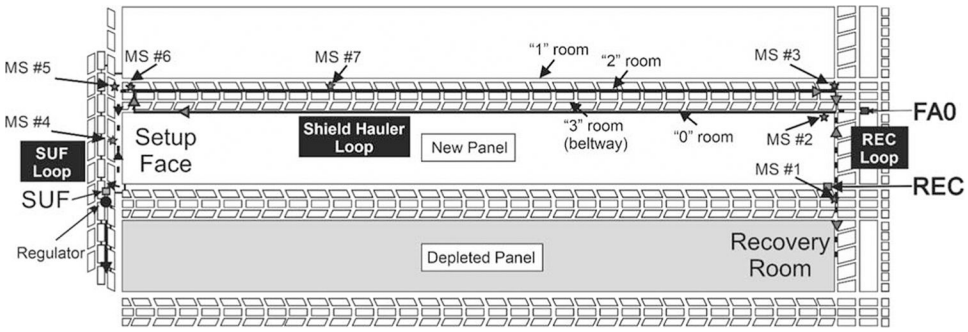

Fig 2.

Location of monitoring station (MS) along the REC loop, shield hauler loop, and SUF loop (not to scale)

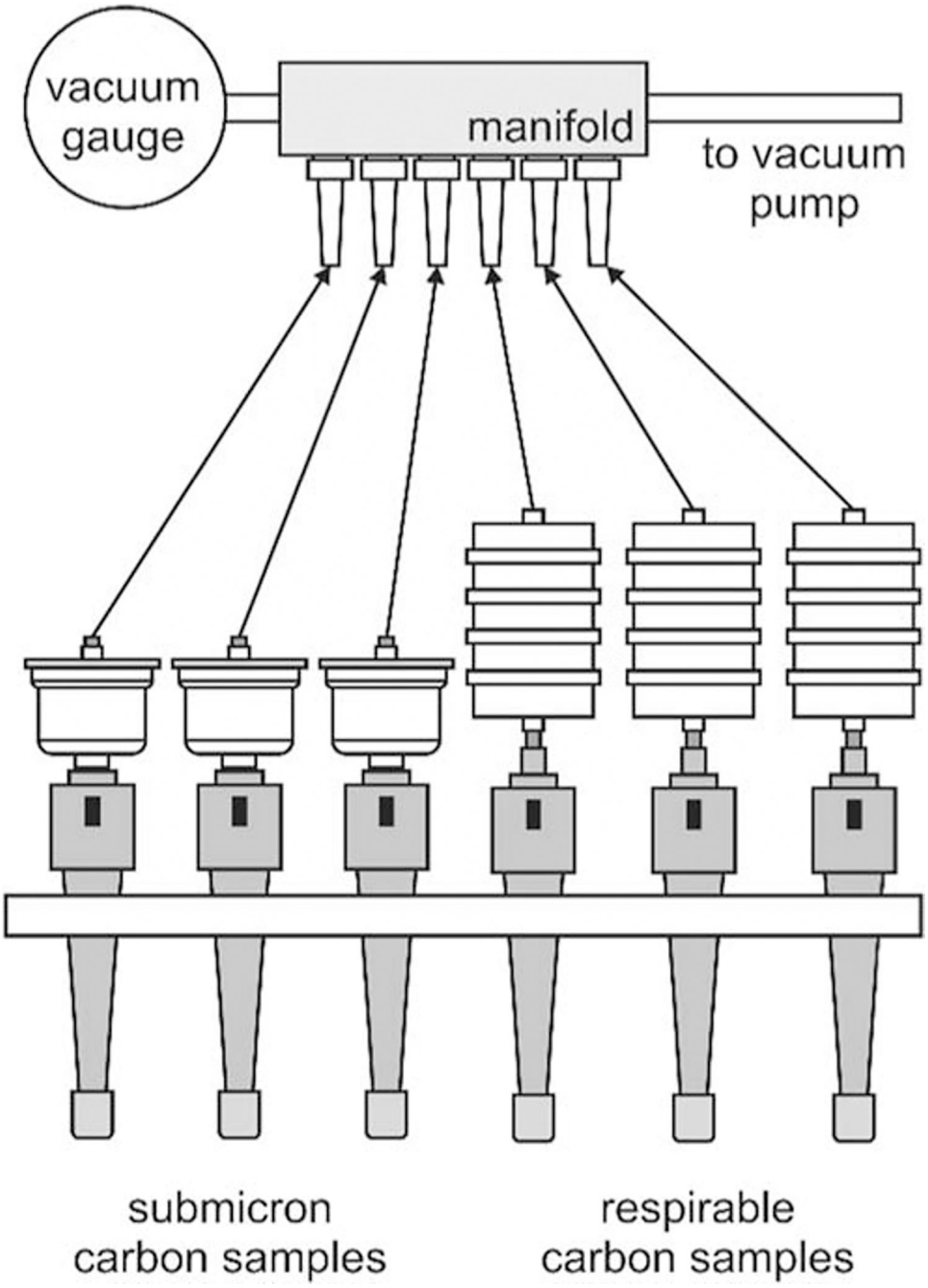

Fig. 3.
Schematic of the sampling trains for submicrometer and respirable samples

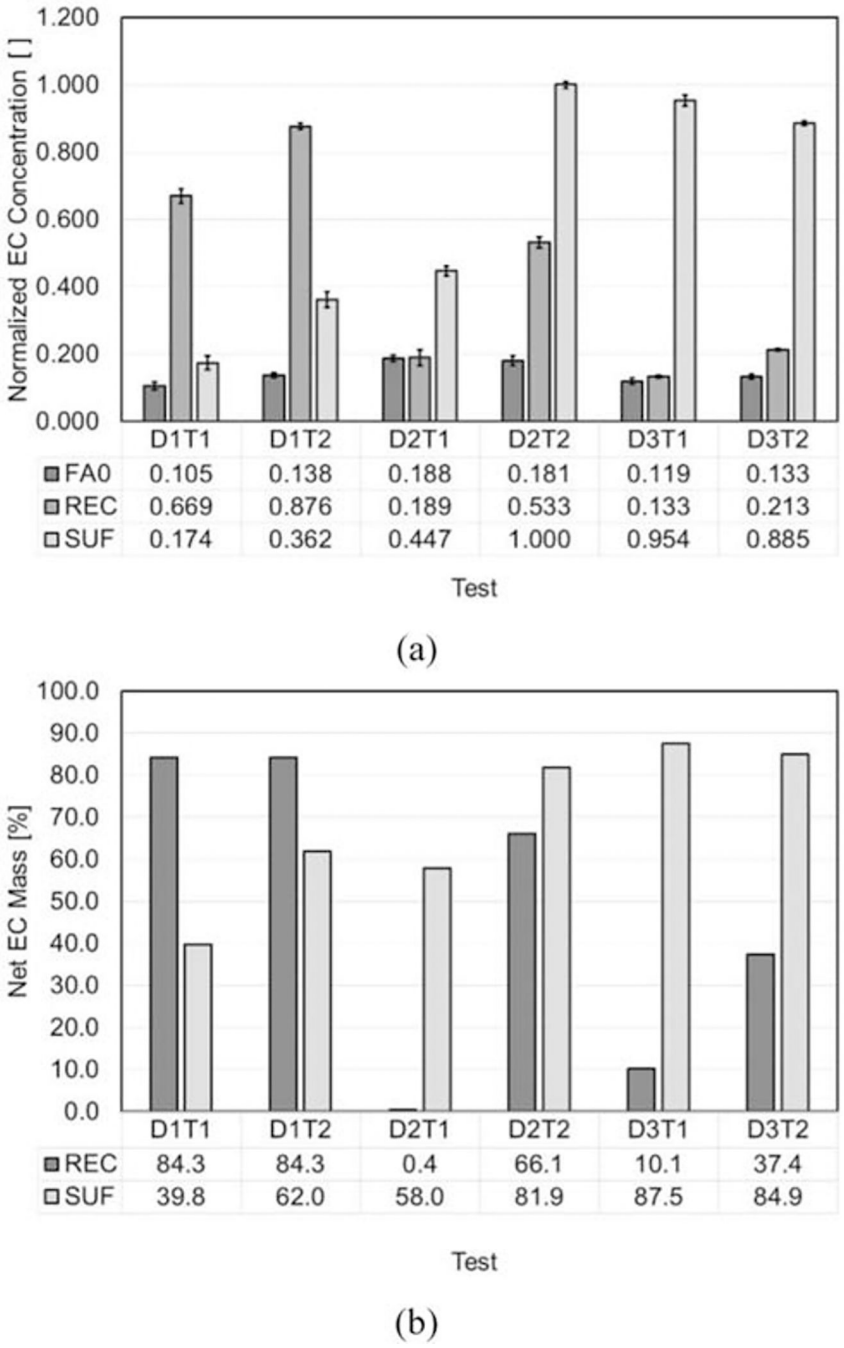

Fig. 4.

a Normalized EC concentrations for FA0, REC, and SUF, and **b** estimated net contribution of the diesel-powered vehicles operated on the REC loop, and on the shield haulage and SUF loops to the concentrations of EC mass flow at REC and SUF, respectively

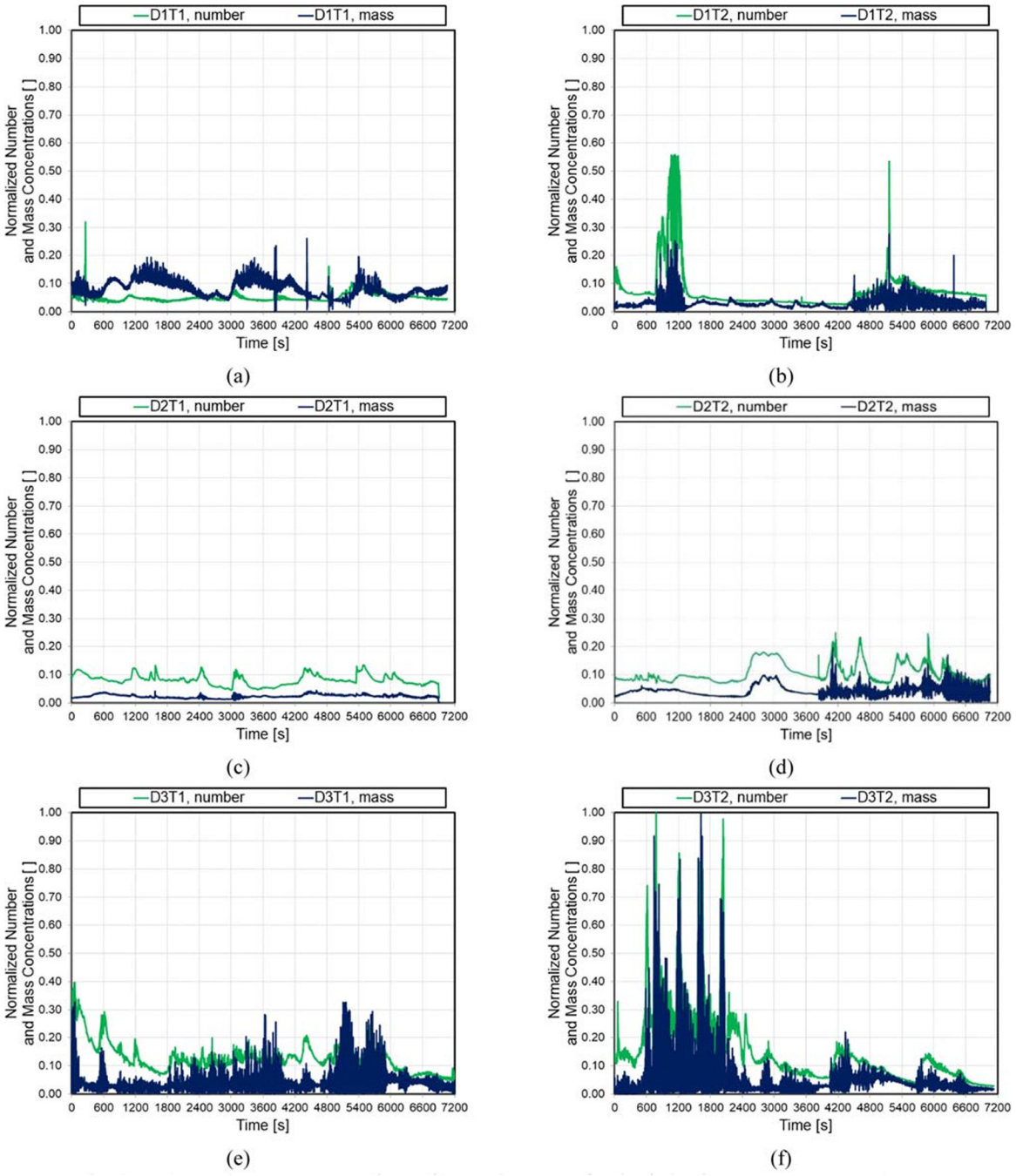

Fig. 5.

Normalized number and mass concentrations of aerosols at SUF for the following tests: (**a**) D1T1, (**b**) D1T2, (**c**) D2T1, (**d**) D2T2, (**e**), D3T1, and (**f**) D3T2

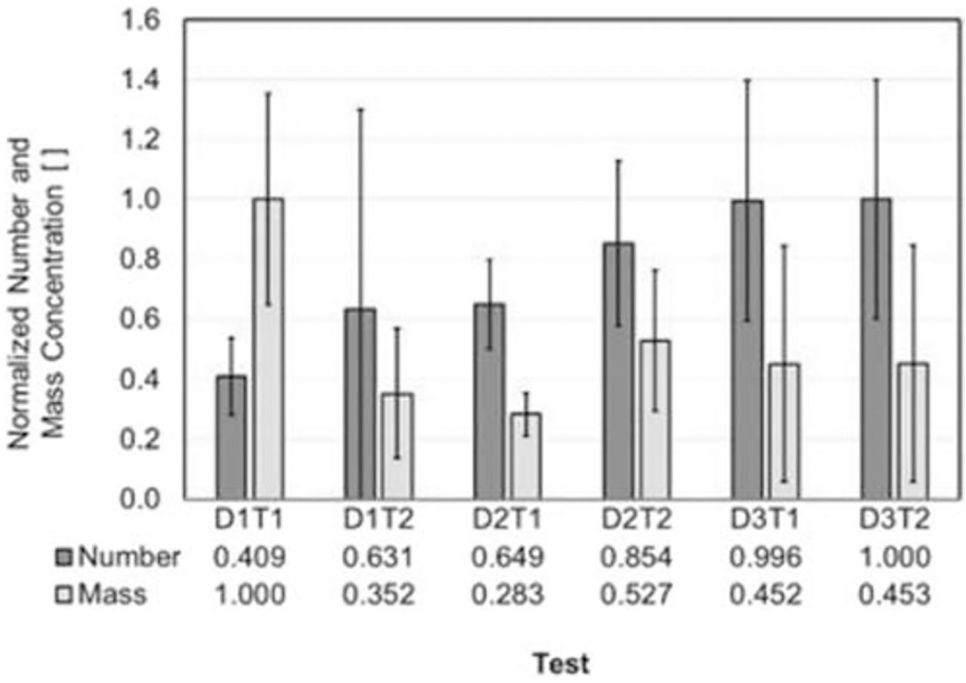

Fig. 6.
Normalized average number and mass concentrations of aerosols at SUF

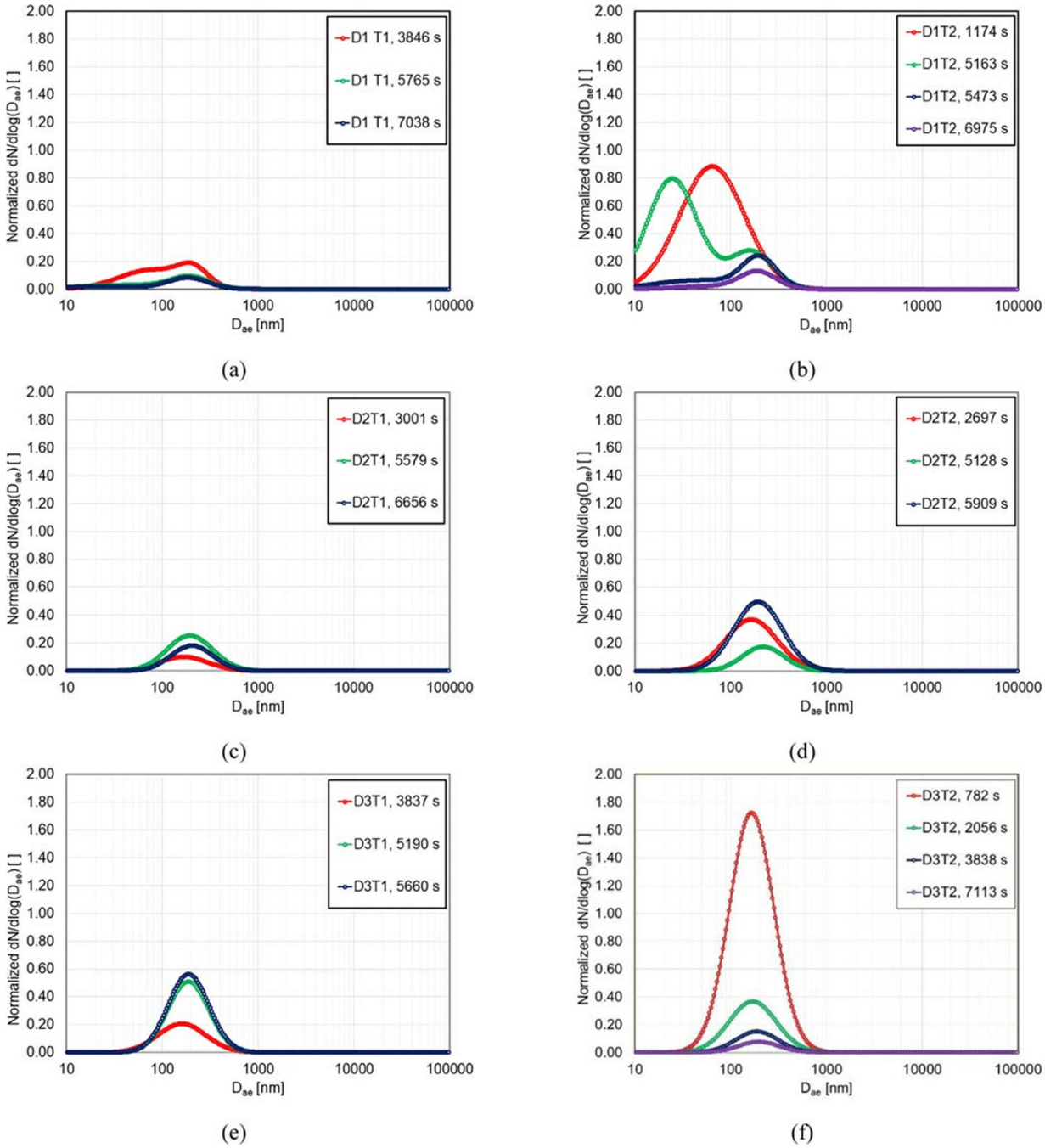

Fig. 7.

Normalized number size distributions for (**a**) D1T1, (**b**) D1T2, (**c**) D2T1, (**d**) D2T2, (**e**) D3T1, and (**f**) D3T2

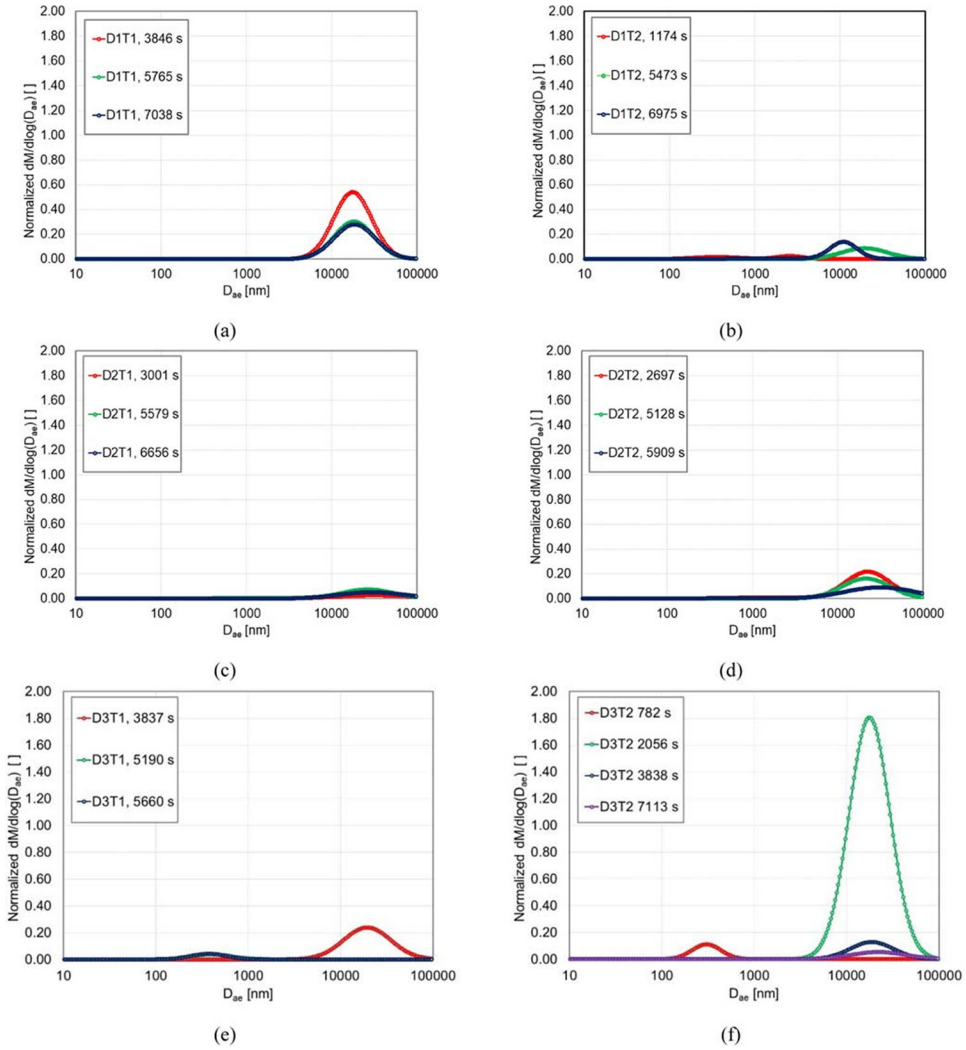

Fig. 8.

Normalized mass size distributions obtained by extrapolating ELPI data for (**a**) D1T1, (**b**) D1T2, (**c**) D2T1, (**d**) D2T2, (**e**) D3T1, and (**f**) D3T2

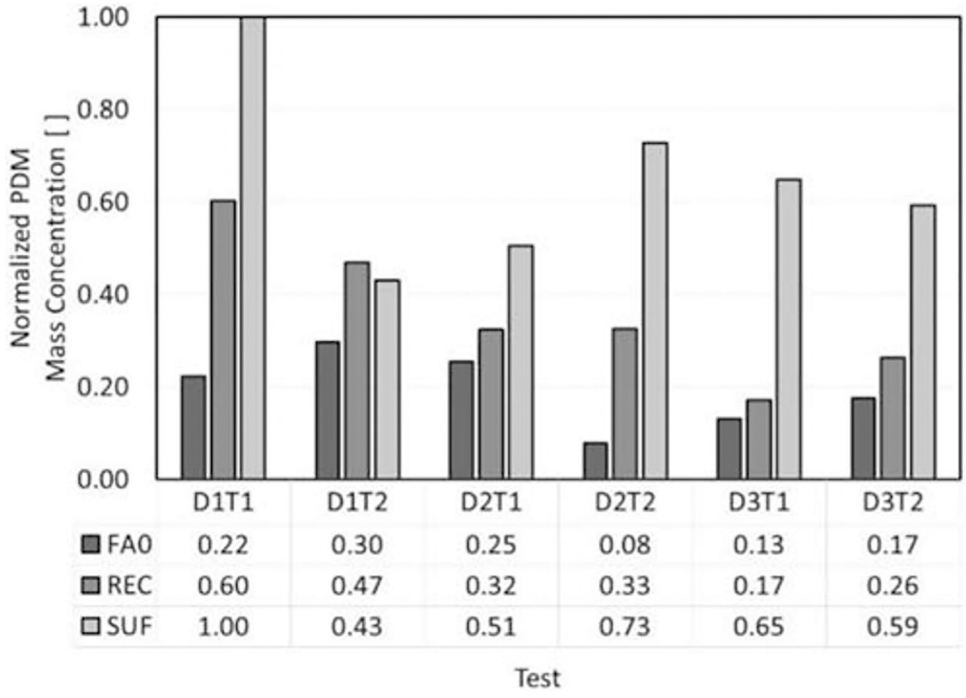

Fig. 9.
Normalized average mass concentrations of the respirable dust at FA0, REC, and SUF

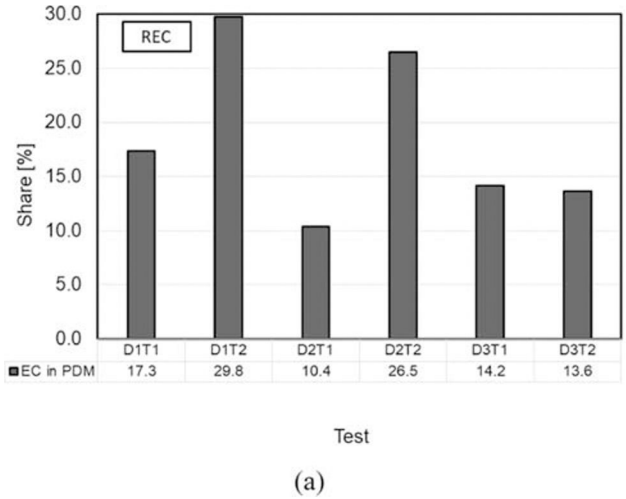

(a)

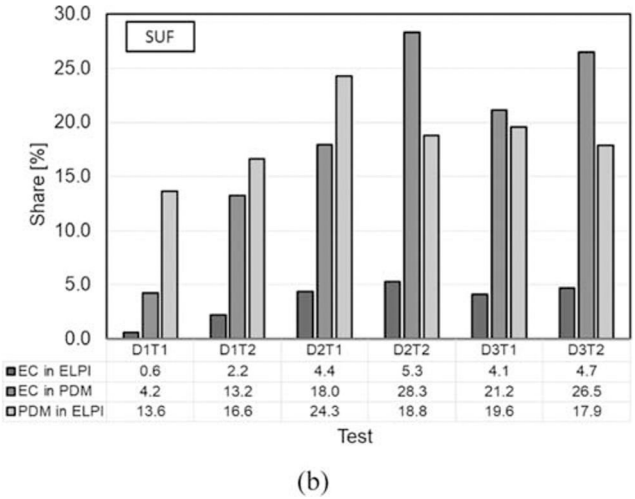

(b)

Fig. 10.

a Share of EC in respirable aerosols for REC. **b** Shares of EC in dust (EC in ELPI), EC in respirable aerosols (EC in PDM), and respirable aerosols in dust (PDM in ELPI) for SUF

Table 1

Properties of diesel fuel used during the study

Fuel property	Test method	ULSD
Heat of combustion [BTU/gal]	ASTM D240	45.3
API gravity @ 15.6 °C [°API]	ASTM D1298	37.1
Cetane number	ASTM D1298	46.4
Sulfur by ultraviolet [ppm]	ASTM D5453	9.0
Flash point, closed cup [°C]	ASTM D93	60.0

Table 2

HD diesel-powered vehicles used during the longwall move

#	Equipment manufacturer	Equipment model	Equipment type	Equipment type 2	MSHA approval number	US EPA Tier	Engine manufacturer and model	Output [kW (hp) @ rpm]
V1	Atlas Copco Wagner, Portland, OR	30X	LHD	HD Pemrissible	7E-B003	Pre	Caterpillar, Peoria, IL, 3306 PCNA	112 (150) @ 2200
V2	J.H. Fletcher & Company, Huntington, WV	Prime mover	Shield hauler	HD Non-Permissible	07-ENA060010	3	Cummins, Columbus, IN, QSB6.7	160 (215) @ 2500
V3	J.H. Fletcher & Company	Prime mover	Shield hauler	HD Non-Permissible	07-ENA060010	3	Cummins QSB6.7	160 (215) @ 2500
V4	Sandvik Mining and Construction, Turku, Finland	LS175	LHD	HD Permissible	07-EPA060001	2	Caterpillar 3126B HEUI	168 (225) @ 2500
V5	Eimco Mining Machinery, Salt Lake City, UT	913	LHD	HD Non-Permissible	07-ENA070006	3	Cummins QSB4.5	127 (170) @ 2500
V6	Eimco Mining Machinery	915	LHD	HD Non-Permissible	7E-B017	Pre	Caterpillar 3306 ATAAC	224 (300) @ 2200

Table 3

Statistical parameters including CMD, σ, and normalized total number concentrations (NTNC) for number distributions of aerosols measured at SUF at selected instants

Test	Instance of time	Mode 1			Mode 2		
		CMD	σ	NTNC	CMD	σ	NTNC
–	s	nm	–	–	nm	–	–
D1T1	3846	77	2.201	0.120	209	1.434	0.048
	5765	49	3.395	0.044	195	1.572	0.039
	7038	27	4.729	0.032	187	1.594	0.038
D1T2	1174	64	2.180	0.751			
	5473	48	2.909	0.078	199	1.504	0.095
	6975	81	2.845	0.028	193	1.529	0.053
D2T1	3001				167	1.797	0.065
	5579				194	1.732	0.153
	6656				204	1.651	0.100
D2T2	2697				163	1.858	0.250
	5128				218	1.648	0.095
	5909				193	1.790	0.315
D3T1	3837				160	1.774	0.129
	5190				187	1.635	0.293
	5660				188	1.633	0.300
D3T2	782				166	1.705	1.000
	2056				171	1.759	0.225
	3838				188	1.655	0.082
	7113				198	1.620	0.040

Table 4

Statistical parameters including MMD, σ, and normalized total mass concentrations (NTMC) for mass distributions of aerosols measured at SUF at selected instants

Test	Instance of time	MODE 1			MODE 2		
		MMD	σ	NTMC	MMD	σ	NTMC
–	s	Nm	–	–	nm	–	–
D1T1	3846				17,680	1.674	0.303
	5765				18,330	1.712	0.178
	7038				18,640	1.744	0.170
D1T2	1174	360	1.928	0.012	2583	1.442	0.010
	5473	460	2.017	0.002	19,410	1.848	0.059
	6975	2809	6.000	0.011	10,990	1.438	0.053
D2T1	3001				31,540	2.708	0.029
	5579	938	3.429	0.004	26,490	2.031	0.056
	6656				29,310	2.404	0.049
D2T2	2697	1370	2.900	0.010	22,660	1.835	0.144
	5128				21,600	1.917	0.115
	5909	729	2.396	0.006	31,370	2.574	0.094
D3T1	3837				19,540	1.795	0.151
	5190	405	1.638	0.020			
	5660	376	1.564	0.020			
D3T2	782	306	1.428	0.043			
	2056				17,740	1.664	1.000
	3838				18,820	1.715	0.075
	7113				22,100	1.973	0.039